ANL/MSD/CP-98660

58930-00-105
58916-00-105

The Effect of Lattice Mismatch on Epitaxial $La_{0.67}Ca_{0.33}MnO_3$ Thin Films

C.J. Eastell, Y.-K. Lin, and D.J. Miller

Materials Science Division
Argonne National Laboratory, Argonne, IL 60439-4845

Submitted for the Proceedings of the 101st American Ceramic Society Meeting, April 25-28, 1999, Indianapolis, IN

Work supported by the U.S. Department of Energy, Division of Basic Energy Sciences-Materials Sciences under contract #W-31-109-ENG-38.

DISCLAIMER

THE EFFECT OF LATTICE MISMATCH ON EPITAXIAL $La_{0.67}Ca_{0.33}MnO_3$ THIN FILMS.

C.J. Eastell, Y.-K. Lin, and D.J. Miller
Materials Science Division, Argonne National Laboratory, Argonne, IL, 60439

ABSTRACT

We present a study of the effect of lattice mismatch on the structure and magneto-transport properties of $La_{0.67}Ca_{0.33}MnO_3$ (LCMO) epitaxial films. Pulsed laser deposition was used to synthesize epitaxial LCMO thin films on $LaAlO_3$ (LAO), $NdGaO_3$ (NGO), $SrTiO_3$ (STO), and MgO substrates. Our results show that the nature of the lattice mismatch and the structure of the substrate governs the microstructure of the film. The microstructure consists of domains of two crystal structures, a pseudo-cubic phase and a monoclinic phase. The monoclinic phase forms as the film relaxes away from the interface, with an orientation dependent on whether the film is under a tensile or compressive in-plane strain. A special case is observed on NGO where the orthorhombic nature of the substrate results in the alignment of the monoclinic phase so that its long axis is in the plane. The observation of an in-plane anisotropy in the magnetoresitance data for LCMO on NGO suggests that the monoclinic phase is important in explaining the magneto-transport properties.

INTRODUCTION

The observation of colossal magnetoresistance behavior (CMR) in perovskite manganite $La_{1-x}(Ba,Ca,Sr)_xMnO_3$ thin films [1] has led to considerable interest in the development of these materials for magnetic sensor and recording applications. A number of studies have been carried out to determine the crystal structure of bulk $La_{1-x}(Ca,Sr)_xMnO_3$ [2-5]. Three different crystal structures have been reported depending on the composition; a F-centered cubic structure ($a \sim 2a_P$) [4], an orthorhombic *pnma* structure ($a \sim \sqrt{2}a_P$, $b \sim 2a_P$, $c \sim \sqrt{2}a_P$) [2,3], and a rhombohedral $R\bar{3}c$ structure ($a \sim \sqrt{2}a_P$, $\alpha \sim 60.4°$) [2,5]. These structures are closely related and the coexistence of two or more phases is a common feature [3].

The structure and microstructure of thin films of the perovskite manganites is made more complex by the effect of strain and structural defects introduced by the lattice mismatch between the film and the substrate. The effect of strain on the magnetic and transport properties of the thin films has been widely discussed [6,7], and it has been shown that in low fields (<1T) a compressive or tensile in-plane strain will increase the magnetoresistance [6,7]. However it is not clear whether this is simply an effect of the strain or the effect of any microstructural changes imposed by the strain. X-ray diffraction (XRD) and transmission electron microscopy (TEM) studies have been carried out for $La_{0.7}Ca_{0.3}MnO_3$ (LCMO) films grown on LAO and STO substrates by Li *et al.* [8] and Lebedev *et al.* [9] respectively. For LCMO on LAO Li *et al.* [8] identified two different structures in their annealed films; a face-centered pseudo-cubic structure ($a \sim 2a_P$) and a pseudo-tetragonal structure ($a \sim \sqrt{2}a_P$, $b \sim \sqrt{2}a_P$, $c \sim 2a_P$). For LCMO on STO Lebedev *et al.* [9] reported that the structure of the film could be indexed to a monoclinic distortion ($a \sim 2a_P$, $b \sim \sqrt{2}a_P$, $c \sim \sqrt{2}a_P$) of the *pnma* phase. They suggest that the preferred orientation of this phase, with the [100] direction parallel to the substrate normal, may be a result of the strain in the film.

In this paper the results of a detailed XRD and TEM study of the microstructure of LCMO films grown on four different substrates (LAO, STO, MgO and NGO) will be presented. The substrates were selected to see if the sign and the magnitude of the strain imposed by the lattice mismatch resulted in changes to the microstructure of the film. Where possible the effect of any

microstructural features on the magnetic and transport properties of the films will also be discussed.

EXPERIMENTAL

LCMO films of composition $La_{0.67}Ca_{0.33}MnO_3$ were grown onto LAO (100), MgO (100), NGO (110) and STO (100) substrates with a pulsed laser deposition (PLD) system using a stoichiometric target and a KrF excimer laser. During the deposition the substrate temperature was 700°C and the oxygen pressure was 600 mτ. Following the deposition the films were annealed at 750°C for 1 hour and then cooled at 2°C/min. In order to minimize the possibility of variation between different depositions, the four samples were grown simultaneously.

The structure of the films was characterized by XRD using 2θ scans and by TEM. TEM was carried out on both plan-view and cross-sectional samples, which were prepared using the standard techniques of grinding and dimpling before being Ar-ion milled at 4 kV. The specimens were examined using a Philips CM30 and a Jeol high-resolution 4000EX TEM, operating at 300 and 400 kV respectively.

Electrical resistance was measured as function of temperature using the standard four point techinique in both zero field and a field of 8T. The magnetoresistance was calculated using $MR = [R_H - R_0]/R_H$. Magnetic measurements were carried out in a squid magnetometer.

RESULTS AND DISCUSSION

X-ray Data

2θ XRD scans were carried out on samples grown on the four different substrates (It should be noted that while LAO, STO and MgO can be indexed as cubic structures, NGO has an orthorhombic structure (a = 0.543nm, b = 0.550nm, c = 0.771nm). In this case the [110] is the substrate normal and the (200) and (110) planes have a d spacing of 0.386nm). The resultant XRD patterns are characteristic of a textured high quality crystalline film. Examples for the films grown on LAO and MgO are shown in figure 1. The peaks are indexed to the (oo*l*) reflections of the face-centered pseudo-cubic ($a \sim 2a_P$) unit cell, however they could just as easily be indexed to the *pnma* orthorhombic unit cell. TEM is required to see which structures are actually present. The out-of-plane lattice parameters were obtained from the 2θ scans and are given in table I. In addition the lattice mismatch between the LCMO and the substrate is also listed. These values were calculated using a lattice parameter of a = 0.3858nm for the bulk LCMO phase [8]. Using the observed out of plane lattice parameter and the bulk lattice parameter, the out-of-plane strain, ε_{zz}, was calculated and is compared in table I to the strain which would be expected if no relaxation had taken place. The expected strain was calculated assuming the in-plane lattice parameters of the film and substrate are the same and the volume of the unit cell is conserved.

From the results in table I four different situations are observed in terms of the degree of strain in the LCMO films. The films grown on STO and LAO are subject to relatively large tensile and compressive in-plane strains respectively, but in both cases the level of the strain is not as high as would be expected if the substrate/LCMO interface was coherent and the film fully strained. For LCMO on NGO and MgO the out-of-plane lattice parameter is close to the bulk value and therefore the film is close to the relaxed state with very little strain. In the case of NGO this is due to the very small lattice mismatch while for MgO it is a result of the lattice mismatch being too large for the film to accommodate the strain and still form a coherent interface. It is important to note though that even with the large lattice mismatch the LCMO film grown on MgO still appears to be textured and of a high crystalline quality.

Transport and Magnetic Properties

Table II summarises the main transport and electrical properties of our LCMO films grown on the different substrates, where T_c is the Curie temperature, T_P is the temperature for the peak resistance in zero field, and T_{MRmax} is the temperature at which the peak magnetoresistance occurs.

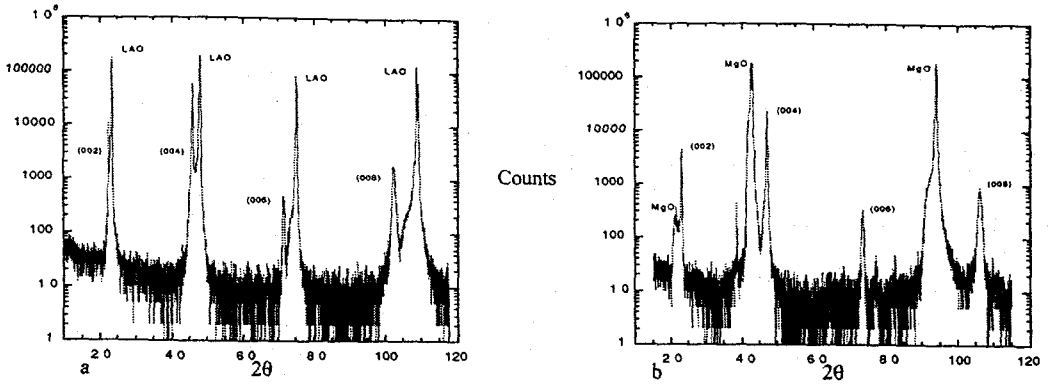

Figure 1. 2θ XRD scans for LCMO films grown on (a) LAO and (b) MgO.

Table I. Comparison of lattice mismatch and strain in the LCMO films

Substrate	Substrate Lattice Parameter (nm)	Lattice Mismatch (%)	Out-of-plane Lattice Parameter (Å)	Measured Out-of-plane Strain, ε_{zz} (%)	Expected Out-of-plane Strain, ε_{zz} (%)
$LaAlO_3$ (100)	0.379	-1.79	3.96	+2.64	+3.62
$NdGaO_3$ (110)	0.386 (a = 0.543, b = 0.550, c = 0.771)	+0.05	~3.86*	~0*	-0.10
$SrTiO_3$ (100)	0.391	+1.33	3.81	-1.24	-2.64
MgO (100)	0.421	+8.36	3.86	+0.05	-16.02

*-Difficult to determine lattice parameter due to overlap of substrate and film peak in 2θ scan.

It should be noted that the structural characterization was carried out on films with a thickness of 120nm, but the magnetoresistance and T_c data were obtained on films with a thickness of 200nm. The most interesting results here are the differences in the properties of the films grown on the LAO and STO substrates. The discrepancy in the T_c can be explained by considering the volume change between the strained LCMO and the bulk LCMO. The unit cell volume for the films can be calculated by assuming that the in-plane parameters of the film and the substrate are the same, and using the out-of-plane parameter obtained from the XRD 2θ scans. The unit cell volume for the bulk material is 5.74×10^{-2} nm^3 while the unit cell volume for the film on LAO is reduced to a value of 5.69×10^{-2} nm^3 and increased to a value of 5.82×10^{-2} nm^3 for the film on STO. The decrease in volume for the film on LAO is equivalent to applying an external hydrostatic pressure, and it has been shown by Hwang *et al.* [10] that applying an external pressure increases the T_c. The volume change for the film on STO is effectively the application of a negative hydrostatic pressure and therefore a lower T_c is observed.

A much higher magnetoresistance is observed for the LCMO film grown on STO compared to the one grown on LAO. It has been shown in low fields (0.5-1T) that strain, either tensile or compressive, increases the magnetoresistance, but as the field is increased to 5T the strain effect is no longer apparent [7]. Our results suggest that in high fields (8T) the nature of the strain and possibly the differences in microstructure resulting from the strain affect the magnetoresistance behavior.

Table II. Transport and magnetic properties of the LCMO films investigated

Substrate	T_p(0T) K	R (T_p) (ohms)	MR (%) $(R_{0T}-R_{8T})/R_{8T}$	T_{Mrmax}	T_c (K)
$LaAlO_3$	270	1027	353	264	270
$NdGaO_3$	265	1432	525	256	265
MgO	266	1435	610	260	265
$SrTiO_3$	250	1725	1095	246	220

TEM Study

Bright field cross-sectional images for the LCMO films grown on NGO and MgO are shown in figure 2. The microstructure of the films appears to be very uniform without the coarse columnar grain growth which has been reported in the literature for thicker films [9]. On this scale the only differences in the films is the high number of dislocations in the LCMO film on MgO. The dislocations (marked by the arrows) are seen to thread their way from the MgO/LCMO interface through to the top surface of the film. The formation of such dislocations is one mechanism by which the strain relaxation occurs in the film. Very few threading dislocations are observed for the films grown on LAO, NGO, and STO as in these cases the strain is small enough to be contained by the lattice.

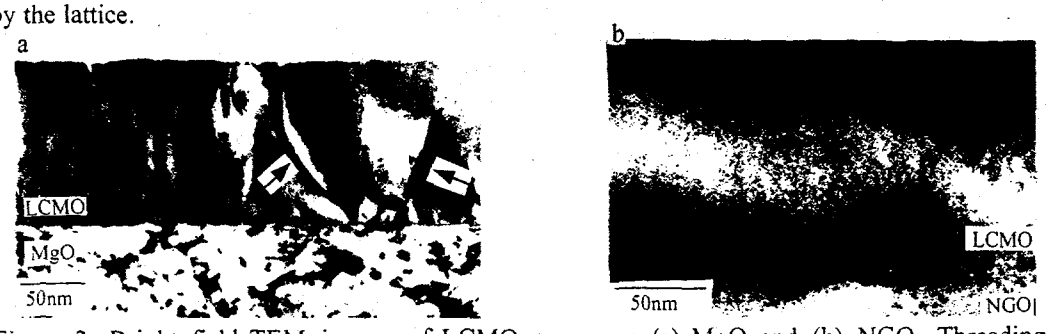

Figure 2. Bright field TEM images of LCMO grown on (a) MgO and (b) NGO. Threading dislocations can be seen in the film on MgO (marked by the arrows).

Using selected area diffraction and microdiffraction techniques two different crystal structures have been observed in all four of the films. The first of these can be indexed as a face-centered pseudo-cubic structure ($a \sim 2a_P$) and diffraction patterns for three different zone axes for this phase are shown in figure 3. This appears to be the same structure reported by Li *et al.* [8] for their LCMO films on LAO. Diffraction patterns for four zone axes from the second structure are shown in figure 4. These patterns can be indexed to a structure which is closely related to the *pnma* orthorhombic phase ($a \sim \sqrt{2}a_P$, $b \sim 2a_P$, $c \sim \sqrt{2}a_P$). High resolution images of this structure, viewed along what would be the [101] direction for the orthorhombic phase, reveal a period doubling along the b axis of ~ 0.77nm. This cannot be accounted for by the *pnma* structure which does not allow the (0k0) reflections with $k = 2n+1$. A similar observation has been made by Lebedev *at al.* [9] who assigned a $P2_1/c$ space group to their structure. In agreement with this our electron diffraction data is consistent with the $P2_1/c$ space group with lattice parameters $a \sim 2a_P$, $b \sim \sqrt{2}a_P$, $c \sim \sqrt{2}a_P$. The fact that all (h00) reflections are allowed for this structure explains the presence of the 0.77nm fringe spacing in high resolution images viewed along the [011] direction.

Figure 5a shows the geometrical relationship between the pseudo-cubic and monoclinic structures. X-ray and electron diffraction data shows that for the cubic structure the epitaxial relationship between the substrate and the film can be described as

$(100)_{LAO}, (110)_{NGO}, (100)_{MGO}, (100)_{STO} \;||\; (100)_{LCMO\ cubic}$

$[001]_{LAO}, [001]_{NGO}, [001]_{MGO}, [001]_{STO} \;||\; [001]_{LCMO\ cubic}$

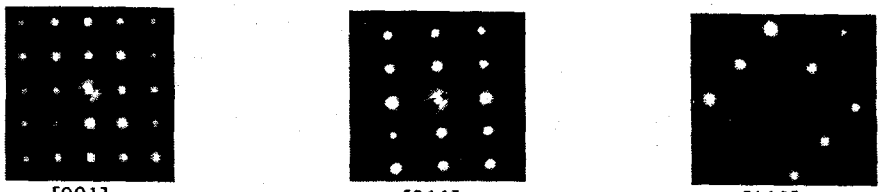

[001] [011] [112]

Figure 3. Three electron diffraction patterns for the face-centered pseudo-cubic structure viewed along the [001], [011] and [112] zone axes.

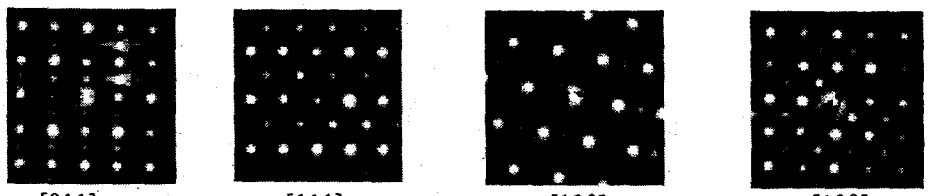

[011] [111] [120] [100].

Figure 4. Four electron diffraction patterns for the monoclinic structure viewed along the [011], [111], [120] and [100] zone axes. Note the odd (h00) type reflections in the [011] zone axis, marked by the arrows.

From figure 5a the (011) plane of the monoclinic phase (shaded in the figure) is equivalent to the (100) in the cubic phase. It can be seen that three different orientations of the monoclinic phase are possible if the epitaxial relationship between LCMO and the substrate is maintained, and these are shown in figure 5b. However, which of the orientations are observed in the film is dependent on the substrate. Typical electron diffraction patterns for the films grown on the different substrates, taken from plan-view specimens with the electron beam parallel to the substrate normal, are shown in figure 6. The small size of the individual monoclinic domains, ranging from a few nm to 500nm, means that each pattern is taken over a large number of domains. For the monoclinic phase in STO we observe only a [100] zone axis in plan-view. This means that the domains are oriented so their long axis is out of the plane. For the film on LAO the plan-view electron diffraction pattern shows the superposition of two 90° oriented $[01\bar{1}]$ zone axes, indicating that the long axis is in the plane and there are two domain orientations related to each other by a 90° rotation. For the film on MgO we observe the superposition of three zones axes, a [100] and two 90° oriented $[01\bar{1}]$ zone axes. This shows that all three structural variants of the monoclinic phase are present for the MgO substrate. Finally for the film on NGO we observe a single $[01\bar{1}]$ zone axis in the plan-view. In this case the long axis is in the plane and oriented parallel to the long axis of the orthorhombic substrate.

Another important observation is that for the strained films on STO and LAO the monoclinic phase is not observed close to the substrate, with lattice fringe images revealing a layer of the pseudo-cubic structure about 10-40nm thick adjacent to the interface (figure 7). High resolution images of the interface for films on both STO and LAO substrates show it to be fully coherent with very few if any misfit dislocations (figure 7b). Our results suggest that as the film relaxes away from the interface the distortion from the pseudo-cubic structure to the monoclinic structure becomes more favorable, and the orientation is determined by whether the in-plane strain is tensile or compressive. Lebedev *et al* [9] also report a similar orientation of the monoclinic phase on STO substrates and suggest that the film relaxes by layers of deformed MnO_6 octahedra preferentially forming along one of the cube planes of the perovskite structure. Our study for films on LAO and STO support their theory that the deformation occurs along the cubic planes which are under compressive strain. The situation is different for the films grown on MgO and NGO. For

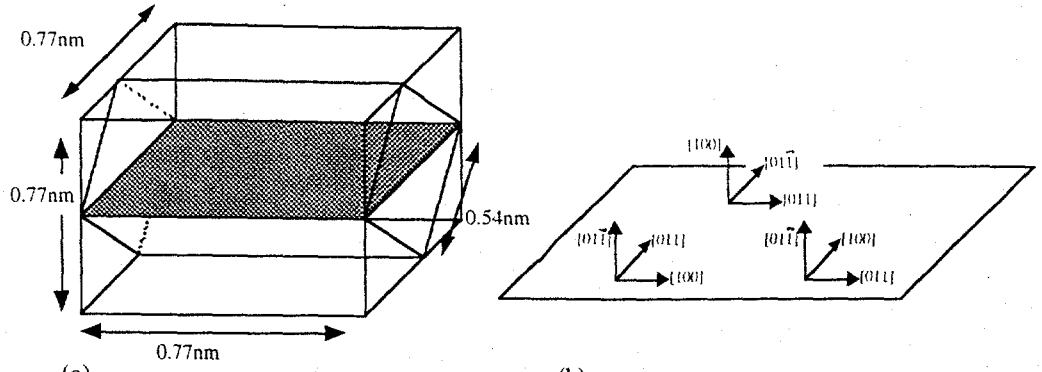

Figure 5. (a) The geometrical relationship between the pseudo-cubic phase and the monoclinic phase. The (011) plane of the monoclinic phase is shaded. (b) The three possible structural orientations of the monoclinic phase.

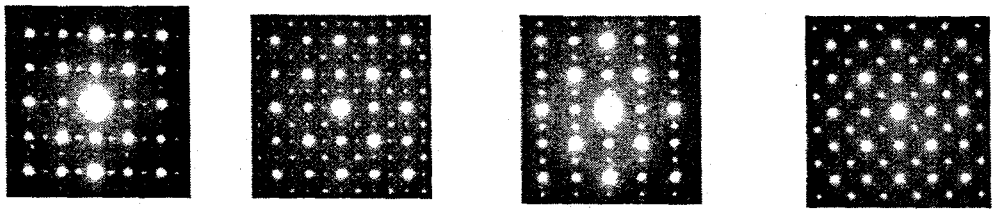

LAO $[01\bar{1}] + [01\bar{1}]\perp$ MgO $[01\bar{1}] + [01\bar{1}]\perp + [100]$ NGO $[01\bar{1}]$ STO [100]

Figure 6. Electron diffraction patterns with the electron beam parallel to the substrate normal. On LAO two domain orientations are present, on MgO three domain orientations are observed , while on NGO and STO single domain orientations are present ($\perp$ indicates a 90° rotation).

MgO the strain has been accommodated for by the formation of the misfit dislocations at the film/substrate interface, (figure8a). This removes the strain induced preferential orientation of the monoclinic phase and as a result all three strucutural variants are observed. For LCMO on NGO the orientation of the monoclinic phase is governed by the orientation of the orthorhombic NGO substrate which forces it to grow so that their long axes are parallel. Interestingly, anisotropy of the transport and MR data is observed for the NGO sample, (figure 9). Two orthogonal in-plane directions were measured corresponding to the a and b axes of the pseudo-cubic cell. In one direction one transition was observed close to T_c but in the other direction a second transition occurred at T = 110K. This result combined with the observation of a single in-plane preferred orientation of the monoclinic phase suggests that the presence of this phase is important in explaining the magnetoresistance properties of these films. In addition the only difference in the microstructure of the LCMO films grown on STO and LAO is the orientation of the monoclinic phase and perhaps this accounts for the higher value of magnetoresistance measured for the STO sample. Further work is currently being undertaken to separate the effects of the two structural phases.

SUMMARY

The nature of the lattice mismatch between the film and the substrate and the structure of the substrate governs the microstructure of the film. Discrepancies in the magnetic and transport properties for the films grown on different substrates are also observed which are likely to be related to the microstructural differences

For all the films two crystal structures were identified, a face-centered pseudo-cubic phase, and a pseudo-orthorhombic phase with a monoclinic distortion. In the strained films the monoclinic phase forms as the film relaxes away from the interface and the sign of the strain induced by the substrate appears to determine its orientation. When there is a tensile in-plane strain (STO) the [100] direction is out of the plane, while for a compressive in-plane strain (LAO) the [011] direction is out of the plane.

It has been shown that by growing the LCMO films on the pseudo-orthorhombic NGO substrate, the structure of the substrate favors the formation of the monoclinic phase and forces it to be textured so that only one domain orientation is observed with the [100] direction in the plane. Such samples should allow the role of the monoclinic phase on the magnetic and transport properties to be investigated.

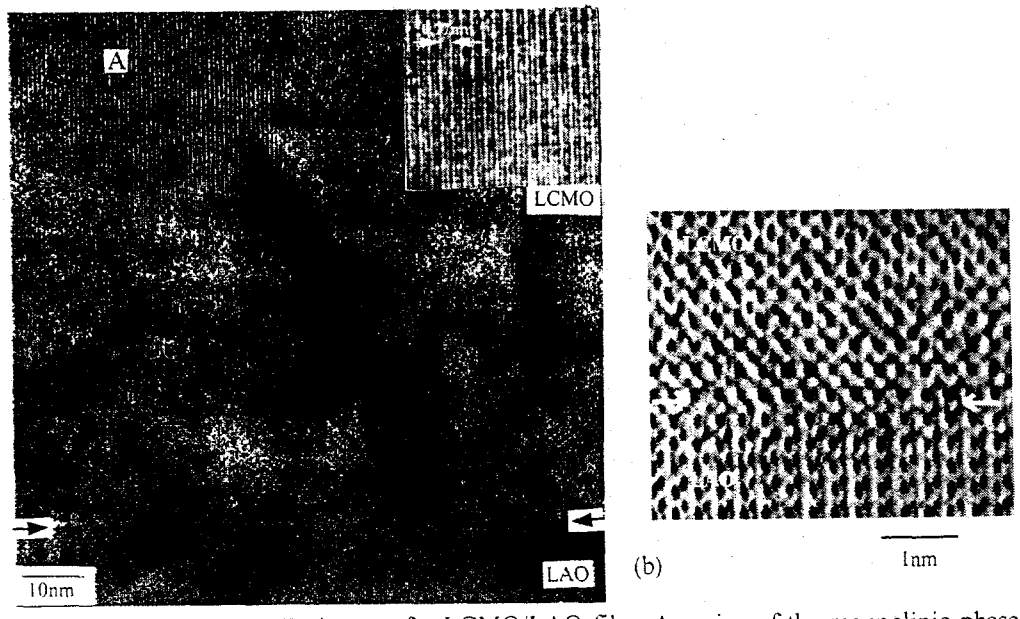

Figure 7. (a) Lattice fringe TEM image of a LCMO/LAO film. A region of the monoclinic phase (A), characterized by the 0.77nm fringe spacing (see inset), is observed away from the interface (arrows). (b) HREM image showing the coherent interface between the LAO substrate and the F-centered pseudo-cubic phase.

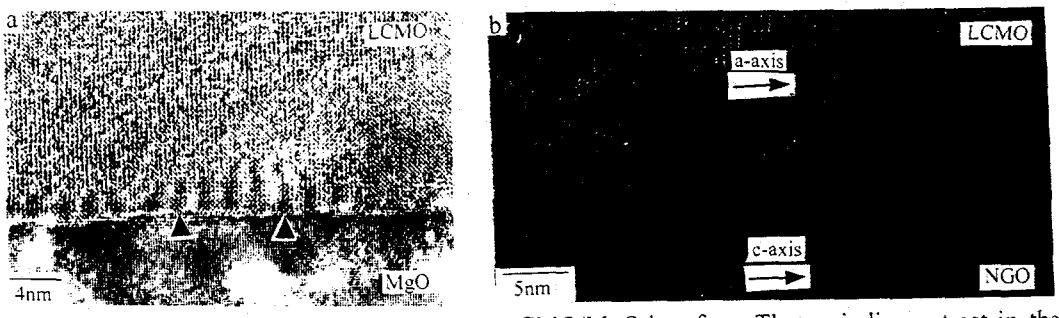

Figure 8. (a) Lattice fringe image showing the LCMO/MgO interface. The periodic contrast in the image is a result of the misfit dislocations (single arrows) which accommodate the large lattice mismatch. (b) Lattice fringe image of the LCMO/NGO interface showing the alignment of the film with the substrate so that their long axes with a fringe spacing of ~ $2a_P$ (labeled in the figure), are parallel.

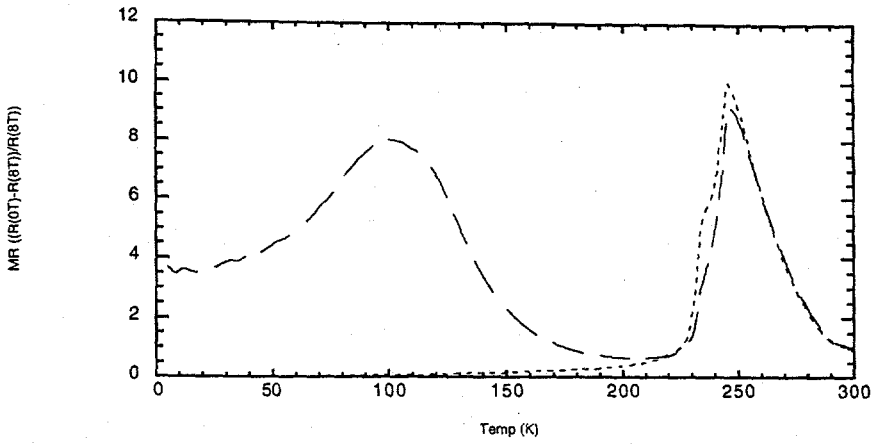

Figure 9. Plot of magnetoresistance against temperature for the LCMO film on NGO, measured along two orthogonal in-plane directions corresponding to the a and b axes of the pseudo-cubic cell.

REFERENCES

1. S. Jin, M. McCormack, T.H. Tiefel, and R. Ramesh, "Colossal Magnetoresistance in La-Ca-Mn-O Ferromagnetic Thin Films", J. Appl. Phys., 76 [10] 6929-6933 (1994).

2. R. Mahendiran, S.K. Tiwary, A.K. Raychaudhuri, T.V. Ramakrishnan, R. Mahesh, N. Rangavittal. and C. Rao, "Structure, Electron-Transport Properties, and Giant Magnetoresistance of Hole-Doped $LaMnO_3$ Systems", Physical Review B, 53 [6] 3348-3358 (1996).

3. P.G. Radaelli, D.E. Cox, M. Marezio, S-W. Cheong, P.E. Schiffer, and A.P. Ramirez, "Simultaneous Structural, Magnetic, and Electronic Transitions in $La_{1-x}Ca_xMnO_3$ with x = 0.25 and 0.5", Physical Review Letters, 75 [24] 4488-4491 (1995).

4. J. Pierre, F. Robaut, S. Misat, P. Strobel, A. Nossov, V. Ustinov, and V. Vassiliev, "Semiconductor-Metal Transition and Magnetoresitance in $(La,Ca)MnO_3$: Experiments and Simple Model", Physica B, 225 214-224 (1996).

5. M.C. Martin, G. Shirane, Y. Endoh, K. Hirota, Y. Moritomo and Y. Tokura, "Magnetism and Structural Distortion in the $La_{0.7}Ca_{0.3}MnO_3$ Metallic Ferromagnet", Physical Review B, 53 [21] 14285-14290 (1996).

6. M.G. Blamire, B.S. Teo, J.H. Durrell, N.D. Mathur, Z.H. Barber, J.L. MacManus-Driscoll, L.F. Cohen, and J.E. Evetts, "Strain-Induced Time Dependent Magnetic Disorder in Ultra-Thin $La_{0.7}Ca_{0.3}MnO_3$ Films, J. Magn Mag. Mat., 191 359-367 (1999).

7. T.Y. Koo, S.H. Park, K.B. Lee, and Y.H. Jeong, "Anisotropic Strains and Magnetoresistance of $La_{0.7}Ca_{0.3}MnO_3$", Appl. Phys. Lett., 71 [7] 977-979 (1997).

8. Y.H. Li, K.A. Thomas, P.S.I.P.N. de Silva, L.F. Cohen, A. Goyal, M. Rajeswari, N.D. Mathur, M.G. Blamire, J.E. Evetts, T. Venkatesen, and J.L. MacManus-Driscoll, "Transmission Electron Microscopy and X-ray Structural Investigation of $La_{0.7}Ca_{0.3}MnO_3$", J. Mater. Res., 13 2161-2169 (1998).

9. O.I. Lebedev, G. Van. Tendeloo, S. Amelinckx, B. Leibold, and H.-U. Habermeier, "Structure and Microstructure of $La_{1-x}Ca_xMnO_{3-d}$ Thin Films Prepared By Pulsed Laser Deposition", Physical Review B, 58 [12] 8065-8074 (1998).

10. H.Y. Hwang, T.T.M. Palstra, S-W. Cheong, and B. Batlogg, "Pressure Effects on the Magnetoresistance in Doped Manganese Perovskites", Physical Review B, 52 [21] 15046-15049 (1995).